

Accurate Approximation of QAM Error Probability on Quasi-static MIMO Channels and its Application to Adaptive Modulation

Fatma Kharrat-Kammoun, Sandrine Fontenelle, and Joseph J. Boutros

fkharrat@enst.fr, sandrine.fontenelle@motorola.com, boutros@enst.fr

Abstract

An accurate approximation for the conditional error probability on quasi-static multiple antenna (MIMO) channels is proposed. For a fixed channel matrix, it is possible to accurately predict the performance of quadrature-amplitude modulations (QAM) transmitted over the MIMO channel in presence of additive white Gaussian noise. The tight approximation is based on a simple Union bound for the point error probability in the n -dimensional real space. Instead of making an exhaustive evaluation of all pairwise error probabilities (intractable in many cases), a Pohst or a Schnorr-Euchner lattice enumeration is used to limit the local theta series inside a finite radius sphere. The local theta series is derived from the original lattice theta series and the point position within the finite multi-dimensional QAM constellation. In particular, we take into account the number of constellation facets (hyperplanes) that are crossing the sphere center. As a direct application to the accurate approximation for the conditional error probability, we describe a new adaptive QAM modulation for quasi-static multiple antenna channels.

Index Terms

Multiple antenna channels, sphere decoding, adaptive modulation, lattice constellations.

I. INTRODUCTION

Since the achievable information rate of conventional systems using a single antenna at both transmitter and receiver is limited by the constellation size, most recent wireless systems use multiple transmit and multiple receive antennas (MIMO channel) to achieve higher data rates [22][9] with a high diversity order [20]. Several techniques have been proposed to improve the performance of these multiple antenna systems regarding the wireless channel conditions, e.g. adaptive modulation [17] and antenna selection [12].

An adaptive modulation technique [10][11] selects the highest information rate (e.g. increase the modulation alphabet size) subject to a double constraint on error rate and the average transmitted power. The selection is conditioned on the instantaneous channel state information within the current frame. Hence, analytical expressions and numerical evaluations for the conditional error probability can be employed to establish an adaptive modulation scheme.

In this paper, we propose an accurate approximation of the conditional error probability in a MIMO system. This tight approximation is then used to design a new adaptive modulation scheme. In the latter, the information rate is adapted per transmit antenna which allows to achieve a high spectral efficiency with an improved adaptation flexibility. Taricco and Biglieri gave the exact pairwise error probability in [18][19] for frequency non-selective multiple antenna systems. The pairwise error probability considered in their paper is the mathematical expectation over all channel realizations. Thus, their closed form expression cannot be used for adaptive modulation. Tarokh *et.al.* proposed in [21] a lower bound of the error probability for a Gaussian channel. This bound is a valid approximation for high rate lattice codes. Since it is a lower bound, the approximation given in [21] cannot provide good performance for adaptive modulation. The tight error probability approximation described in this paper is conditioned on a fixed channel realization. The proposed method does not require an intractable evaluation of all pairwise error probabilities due to a judicious choice via Pohst/Schnorr-Euchner enumeration of dominant neighbors inside a sphere centered around a constellation point.

The paper is organized as follows. Section II introduces the notations and the channel model. The accurate approximation of the conditional error probability is given in Section III. Section IV describes the new adaptive QAM modulation scheme for multiple antenna channels. Conclusions and perspectives are drawn in the last section.

II. SYSTEM MODEL AND LATTICE REPRESENTATION

We consider a digital transmission system with n_t transmit antennas and n_r receive antennas. The channel is assumed to be frequency non-selective and quasi-static. The $n_t \times n_r$ MIMO channel matrix $\mathbf{H} = [h_{ij}]$ is constant during T_c channel uses, where the integer T_c is the channel coherence time. In the latter, one time unit is equal to one transmission period. As usual, the coefficients h_{ij} are independent zero-mean unit-variance complex Gaussian variables that take independent values each T_c periods. For one channel use, the input-output model is

$$\mathbf{r} = \mathbf{s}\mathbf{H} + \boldsymbol{\nu}, \quad (1)$$

where \mathbf{r} is the length n_r receive complex vector, \mathbf{s} is the length n_t transmit vector and $\boldsymbol{\nu}$ is an additive white Gaussian noise. The transmitted symbol s_k belongs to a M_k -QAM modulation [16], $k = 1 \dots n_t$. The n_t QAM constellations are not necessary identical, their Cartesian product is denoted C_{QAM} .

Without loss of generality and for the sake of simplicity, we assume that $n_t = n_r$. The study is similar in the asymmetric channel case when $n_r \geq n_t$. The performance study of the quasi-static multiple antenna model in (1) is carried out thanks to lattices and sphere packings theory [6]. The paragraph below gives a brief summary to point lattices and can be skipped by readers who are familiar with group/lattice representation and the geometry of numbers.

Let K be a field, mainly $K = \mathbb{R}$ the field of real numbers, or $K = \mathbb{C}$ the field of complex numbers. Let $A \subset K$ be a ring, mainly $A = \mathbb{Z}$ the ring of integers, or $A = \mathbb{Z}[i]$ the ring of Gaussian integers. A *lattice* $\Lambda \subset K^n$, also called a point lattice, is a free A -module of rank n in K^n . An element belonging to Λ is called a point or equivalently a vector. Any point $\mathbf{x} = (x_1, x_2, \dots, x_n) \in \Lambda$ can be written as an integer linear combination of n points

$$\mathbf{x} = \sum_{i=1}^n z_i \mathbf{v}_i,$$

where $\{\mathbf{v}_i\}$ is an A -basis of Λ , $v_{ij} \in K$, and $z_i \in A$. The $n \times n$ matrix built from a basis is a *generator matrix* for Λ . In line convention, let $\mathbf{G} = [v_{ij}]$, then a lattice point is written as $\mathbf{x} = \mathbf{z}\mathbf{G}$, where $\mathbf{z} \in A^n$. The squared norm of \mathbf{x} is defined as $\|\mathbf{x}\|^2 = \mathbf{x}\mathbf{x}^\dagger = \sum_{i=1}^n |x_i|^2$, where $|x_i|^2$ is defined by the product of x_i with its conjugate in K . In the real case, a lattice Λ is associated to a definite positive quadratic form $Q(\mathbf{x}) = \mathbf{x}\mathbf{x}^t = \mathbf{z}\mathbf{G}\mathbf{G}^t\mathbf{z}^t$, where t denotes the transpose operation. The product $\mathbf{G}\mathbf{G}^t$ is called a *Gram matrix*. Since Λ has full rank, the determinant of the Gram matrix is positive. The fundamental volume of the lattice is defined by $vol(\Lambda) = |\det(\mathbf{G})|$, it is the volume of the *fundamental parallelepiped* \mathcal{P} surrounded by the basis vectors \mathbf{v}_i

$$\mathcal{P}(\Lambda) = \{\mathbf{x} \in \mathbb{R}^n \mid \mathbf{x} = \sum_{i=1}^n \alpha_i \mathbf{v}_i, 0 \leq \alpha_i < 1\}.$$

Multiple antenna channels admit a complex lattice representation as random $\mathbb{Z}[i]$ -modules. In this paper, we will mainly use their real representation. As an illustrative example for deterministic highly structured lattices, Fig. 1 shows the structure of the famous hexagonal lattice A_2 . A generator matrix for A_2 is

$$\mathbf{G}(A_2) = \begin{bmatrix} 1 & 0 \\ 1/2 & \sqrt{3}/2 \end{bmatrix}.$$

Some of the important lattice parameters are also depicted in Fig. 1. The *minimum Euclidean distance* between distinct lattice points is denoted by $d_{Emin}(\Lambda) = 2\rho$, where ρ is the sphere packing radius associated to Λ as shown in the upper left part of Fig. 1. Each point has τ neighboring points located at

minimum distance. For A_2 , we have $\tau = 6$. From a sphere packing point of view, the number τ of nearest neighbors is also called *kissing number*. Consider $\mathbf{x} \in \Lambda$ and delimit its neighborhood by mediating hyperplanes between \mathbf{x} and all other lattice points. The obtained region is called *Voronoi cell* or Dirichlet region

$$\mathcal{V}(\mathbf{x}) = \{\mathbf{y} \in \mathbb{R}^n \mid |\mathbf{y} - \mathbf{x}| < |\mathbf{y} - \mathbf{x}'|, \forall \mathbf{x}' \in \Lambda\}.$$

For A_2 , $\mathcal{V}(\mathbf{x})$ has six facets obtained by the six mediating segments with the nearest points. Since a lattice is a discrete subgroup of K^n , the distribution of Euclidean distances does not depend on \mathbf{x} . Take $\mathbf{x} = \mathbf{0}$, in Fig. 1 notice that lattice points belong to shells centered on the origin. The Euclidean distance distribution is given by the radius of lattice shells and their population (number of points in a shell). Similar to the Hamming weight distribution of an error-correcting code defined over a finite field, the *theta series* $\Theta_\Lambda(z)$ of Λ describes its Euclidean distance distribution

$$\Theta_\Lambda(z) = \sum_{\mathbf{x} \in \Lambda} q^{\|\mathbf{x}\|^2} = 1 + \tau q^{4\rho^2} + \dots, \quad (2)$$

where $q = e^{i\pi z}$, and z is a complex variable. The theta series of highly structured lattices (e.g. integral lattices) is known for low dimensions [6]. Some simple examples are

$$\Theta_{\mathbb{Z}}(z) = \sum_{m=-\infty}^{+\infty} q^{m^2} = 1 + 2q + 2q^4 + 2q^9 + 2q^{16} + \dots = \theta_3(z),$$

where $\theta_3(z)$ is a Jacobi theta function. It is trivial to show that $\Theta_{\mathbb{Z}^n}(z) = \Theta_{\mathbb{Z}}(z)^n = \theta_3(z)^n$. Also, the theta series of the translated lattice $\mathbb{Z} + 1/2$ is

$$\Theta_{\mathbb{Z}+1/2}(z) = \sum_{m=-\infty}^{+\infty} q^{(m+1/2)^2} = 2q^{1/4} + 2q^{9/4} + 2q^{25/4} + \dots = \theta_2(z),$$

where $\theta_2(z)$ is also a Jacobi theta function. Finally, the theta function of the hexagonal lattice is given by

$$\Theta_{A_2}(z) = \sum_{\mathbf{x} \in \Lambda} q^{Q(\mathbf{x})} = \theta_3(z)\theta_3(3z) + \theta_2(z)\theta_2(3z) = 1 + 6q + 6q^3 + 6q^4 + 12q^7 + \dots,$$

where $Q(\mathbf{x})$ is the quadratic form associated to A_2 . The reader can check that the theta series exactly describes A_2 shells population and radius as illustrated in Fig. 1. If Λ is a random lattice, then $\Theta_\Lambda(z)$ or at least all its terms up to q^C can be determined using the *Short Vectors* algorithm that solves $Q(\mathbf{x}) \leq C$ [14][15][5]. Before terminating this tutorial section, let us introduce two more parameters related to the density of the lattice sphere packing. The *density* Δ of a lattice is defined by

$$\Delta = \frac{\text{volume of a packing sphere of radius } \rho}{\text{volume of a Voronoi cell}} = \frac{V_n \rho^n}{\text{vol}(\Lambda)},$$

where $V_n = \pi^{n/2}/\Gamma(n/2 + 1)$, and $\Gamma(x)$ is the classical Gamma function. The center density δ is defined by normalizing Δ , i.e. $\delta = \Delta/V_n$. The density of Λ and its error rate performance in presence of additive noise are also related to its *fundamental gain* (also known as Hermite constant) defined by [6][8]

$$\gamma(\Lambda) = \frac{d_{Emin}^2(\Lambda)}{n^{1/2} \sqrt{\text{vol}(\Lambda)}} = 4^{n/2} \sqrt{\delta}. \quad (3)$$

Now let us resume with the lattice representation of a multiple antenna channel. The product $\mathbf{x} = \mathbf{s}\mathbf{H}$ in (1) is interpreted as a point in the Euclidean space \mathbb{R}^n , $n = 2n_t = 2n_r$. The point \mathbf{x} belongs to a real lattice Λ of rank n . The $n \times n$ generator matrix $\mathbf{G} = [g_{ij}]$ of Λ is the real version of \mathbf{H}

$$\left\{ \begin{array}{l} g_{2i,2j} = \Re(h_{i,j}) \\ g_{2i+1,2j} = -\Im(h_{i,j}) \\ g_{2i,2j+1} = \Im(h_{i,j}) \\ g_{2i+1,2j+1} = \Re(h_{i,j}) \end{array} \right. \quad (4)$$

Since \mathbf{s} is limited to $C_{\text{QAM}} \subset \mathbb{Z}^n$, then $\mathbf{x} \in C^{\mathbf{H}} \subset \Lambda$, where $C^{\mathbf{H}}$ is a finite set of Λ called a lattice constellation or lattice code. When C_{QAM} is square, the shape of $C^{\mathbf{H}}$ is given by the parallelotope \mathcal{P} , i.e. $C^{\mathbf{H}}$ and \mathcal{P} are homothetic. The reader should notice that a M_k -QAM modulation is defined as a rectangular subset of \mathbb{Z}^2 and that any scaling factor or any translation generates an equivalent set. The

cardinality of the lattice constellation $C^{\mathbf{H}}$ is $\prod_{k=1}^{n_t} M_k$. The spectral efficiency of the uncoded QAM system is $\sum_{k=1}^{n_t} \log_2(M_k)$ bits per channel use.

At the receiver side, it is assumed that perfect channel state information (perfect CSI) is available. CSI is not required at the transmitter side. Finally, a maximum-likelihood detector based on a sphere decoder is applied [23][1][3] to accomplish a low complexity detection.

III. ACCURATE APPROXIMATION OF ERROR PROBABILITY

The lattice representation of a multiple antenna channel converts the MIMO model given in (1) into a simple additive white Gaussian noise (AWGN) channel model $\mathbf{r} = \mathbf{x} + \boldsymbol{\nu}$. For a given random lattice Λ generated by a fixed channel matrix \mathbf{H} , let $Pe(\Lambda)$ denote the point error probability associated to the infinite set Λ and let $Pe(C^{\mathbf{H}})$ denote the average point error probability associated to the finite constellation $C^{\mathbf{H}}$. Trivial geometrical properties leads to the inequality $Pe(C^{\mathbf{H}}) \leq Pe(\Lambda)$.

Due to the geometrical uniformity of Λ , the error probability $Pe(\Lambda)$ does not depend on the transmitted point, e.g. $Pe(\Lambda) = Pe_{|\mathbf{0}} \leq \sum_{\mathbf{x} \neq \mathbf{0}} P(\mathbf{0} \rightarrow \mathbf{x})$, where $P(\mathbf{x} \rightarrow \mathbf{y})$ is the classical notation for the pairwise error probability and $Pe_{|\mathbf{x}}$ is the error probability conditioned on the transmission of \mathbf{x} . On the contrary, $C^{\mathbf{H}}$ is not geometrically uniform. To find its exact error probability, we should evaluate $Pe_{|\mathbf{x}}$ for all $\mathbf{x} \in C^{\mathbf{H}}$, and then average by $Pe(C^{\mathbf{H}}) = \frac{1}{|C^{\mathbf{H}}|} \sum_{\mathbf{x} \in C^{\mathbf{H}}} Pe_{|\mathbf{x}}$.

For example, when $n_t = 4$ and $M_k = 16$ for all k , a classical Union bound would cost 65536×65535 Euclidean distance evaluations. To reduce the complexity, we propose in the following a method which yields a very accurate approximation for the error rate of $C^{\mathbf{H}}$ at a negligible complexity price.

It is well known in lattice theory [6] that integrating a Gaussian noise over a Voronoi region to get the error probability is an extremely difficult task. If integration is to be done numerically and if a random lattice is considered, one can imagine to determine a complete description of the Voronoi region via the Diamond Cutting Algorithm (Viterbo and Biglieri 1996 in [24]) and then integrate using the Gaussian

distribution. Unfortunately, the task is still extremely complex. The integration must be done for all points in the case of a finite constellation, or at least a large number of points if symmetry exists. Hence, error rates $Pe(\Lambda)$ and $Pe(C^{\mathbf{H}})$ cannot be exactly computed by numerical integration that avoids Monte Carlo simulation. Under the assumption that all facets of the Voronoi region are created by the first lattice shell, we have

$$Pe(C^{\mathbf{H}}) \leq Pe(\Lambda) \leq \tau(\Lambda) \times Q\left(\frac{d_{Emin}(\Lambda)}{2\sigma}\right). \quad (5)$$

In the above inequality, $\tau(\Lambda)$ is the kissing number, $d_{Emin}(\Lambda)$ is the minimum Euclidean distance, and σ^2 is the one-dimensional real noise variance. The situation in which the right inequality of (5) is valid corresponds to dense lattice packings, i.e. the fundamental gain $\gamma(\Lambda)$ given in (3) is greater than 1 [6][8].

Unfortunately, random lattices generated by \mathbf{H} are not necessarily dense, especially for $n_t \leq 4$ as illustrated in Fig. 2. Thus, in the general case, the theta series of Λ is needed to derive an upper bound for $Pe(\Lambda)$. In practice, during numerical evaluations, the theta series defined in (2) will be truncated to a limited number of shells around the transmitted point. This truncation yields precise numerical results because the lattice is transmitted on a Gaussian channel where pairwise error probability decreases exponentially with respect to Euclidean distance.

When square QAM modulations are applied on the transmit antennas, (5) becomes (6) (see [4]),

$$Pe(C^{\mathbf{H}}) \leq Pe(\Lambda) \leq \tau(\Lambda) \times Q\left(\sqrt{\frac{3 \times \sum_{i=1}^{n_t} \log_2 M_i}{n_r \times \sum_{i=1}^{n_t} (M_i - 1)} \times \frac{E_b}{N_0} \times \gamma(\Lambda)}\right) \quad (6)$$

where E_b/N_0 denotes the average received SNR per bit.

Now, let us describe how shall we handle the non geometrically uniform set $C^{\mathbf{H}}$ in order to reduce the computational complexity with respect to the Union bound. With this method, we aim at finding a precise approximation for the point error rate, although not in closed-form. Consider a 16-QAM constellation transmitted on a Gaussian channel. It can be partitioned into 3 subsets: 4 points in the middle (I_0), 8

non-corner points on the facets (I_1), and 4 points on its corners (I_2). There are 3 different error rates, one for each subset. The total point error rate is obtained by $4/16Pe(I_0) + 8/16Pe(I_1) + 4/16Pe(I_2)$, no need to compute 16 error rates corresponding to 16×15 distance evaluations. Now, generalize the previous idea to a dimension $n \geq 2$, where the constellation is not cubic shaped (\mathbf{H} is random).

For a given constellation point $\mathbf{x} = \mathbf{sH} = \mathbf{zG}$, the local theta series, *i.e.* the distance distribution of points surrounding \mathbf{x} and belonging to $C^{\mathbf{H}}$, depends on \mathbf{x} . This observation is noticed in Fig. 3 that represents points of a lattice constellation carved from a lattice $\Lambda \subset \mathbb{R}^2$. The local theta series of indicated points, which are black filled up to a square radius R , are not identical.

More precisely, the distribution of Euclidean distances around \mathbf{x} depends on the position of \mathbf{x} in $C^{\mathbf{H}}$. If \mathbf{x} does not belong to the boundary of $C^{\mathbf{H}}$ (the point belongs to the interior of the constellation) then boundary effects can be neglected and the local theta series is well approximated by the theta series of Λ . Otherwise, if the point \mathbf{x} is located on the boundary of $C^{\mathbf{H}}$, then the local theta series is derived by translating the original one around \mathbf{x} and deleting all lattice points that do not belong to $C^{\mathbf{H}}$. To do so, we partition the constellation into $n + 1$ subsets

$$C^{\mathbf{H}} = \bigcup_{\ell=0}^n I_{\ell}, \quad (7)$$

where I_{ℓ} contains lattice points located on the intersection of ℓ facets in $C^{\mathbf{H}}$. The subset I_0 is the interior of the constellation. Notice that $\mathbf{x} = \mathbf{zG} \in I_{\ell}$ is equivalent to \mathbf{z} belonging to the intersection of ℓ facets in $C_{\text{QAM}} \subset \mathbb{Z}^n$. Following (7), the error probability of the constellation becomes

$$Pe(C^{\mathbf{H}}) = \sum_{\ell=0}^n p_{\ell} Pe(I_{\ell}). \quad (8)$$

The weighting factor p_{ℓ} is the probability that a point of $C^{\mathbf{H}}$ belongs to the subset I_{ℓ} , and $Pe(I_{\ell})$ is the error probability associated to I_{ℓ} . The probability $Pe(I_{\ell})$ is obtained by averaging over all points $\mathbf{x} \in I_{\ell}$, since the conditional probability $Pe_{|\mathbf{x}}$ depends on the local position of \mathbf{x} . In the sequel, we describe

how an accurate approximation of (8) can be obtained. The accuracy of the analytical approximation is validated by comparing it to computer simulations as illustrated in Figs. 4 and 5.

A. Evaluation of the probability p_ℓ

For simplicity reasons, only square QAM constellations are considered. Thus, any M -QAM is written as the Cartesian product of Pulse Amplitude Modulation M -QAM = $(\sqrt{M}$ -PAM)². The generalization to rectangular and cross bi-dimensional constellations is straightforward. Also, it is assumed that QAM symbols transmitted on the MIMO channel have the same a priori probability.

- **All antennas transmit the same QAM set**

The probability for a point component to be located on the edge of the one-dimensional PAM is $2/\sqrt{M}$.

Since ℓ components out of n must be on the PAM boundaries, then it is trivial to show that

$$p_\ell = \binom{n}{\ell} \left(\frac{2}{\sqrt{M}} \right)^\ell \left(1 - \frac{2}{\sqrt{M}} \right)^{n-\ell}. \quad (9)$$

- **Antennas transmit general QAM sets (not necessarily identical)**

The number ℓ of constellation facets to which a point $\mathbf{x} = \mathbf{zG}$ belongs in \mathbb{R}^n is decomposed as

$$\ell = \sum_{i=1}^n \ell_i, \quad (10)$$

$\ell \in [0..n]$ and $\ell_i \in \{0, 1\}$. The integer ℓ_i is set to 1 if z_i location is on the PAM boundary . Notice that

z_i , $i = 1 \dots n$, belongs to a PAM real constellation of size $\sqrt{M_{[(i+1)/2]}}$, where M_k is the size of the k^{th}

bi-dimensional QAM set, $1 \leq k \leq n_t = n/2$. For a given value of ℓ , let $L_{\ell,j} = (\ell_1^j \dots \ell_i^j \dots \ell_n^j)$ denote a

length n binary vector whose components satisfy the sum condition (10), $1 \leq j \leq \binom{n}{\ell}$. Then, it is

easy to show that

$$p_\ell = \sum_{L_{\ell,j}} \prod_{i=1}^n \left(\frac{2}{\sqrt{M_{[(i+1)/2]}}} \right)^{\ell_i^j} \left(1 - \frac{2}{\sqrt{M_{[(i+1)/2]}}} \right)^{1-\ell_i^j}. \quad (11)$$

The above expression reduces to (9) when identical QAM sets are used on the MIMO channel.

B. Evaluation of the subset error probability $Pe(I_\ell)$

We establish an upper bound for $Pe(I_\ell)$ using the local theta series. Computer simulations given below show the tightness of this bound which is due to the simple AWGN model defined by $\mathbf{r} = \mathbf{x} + \boldsymbol{\nu}$.

The error probability $Pe(I_\ell)$ used in (8) can be written as:

$$Pe(I_\ell) = \frac{1}{|I_\ell|} \sum_{\mathbf{x} \in I_\ell} Pe_{|\mathbf{x}}, \quad (12)$$

Let $S_{\mathbf{x},i} = \{\mathbf{y} \in C^{\mathbf{H}} | d_E(\mathbf{x}, \mathbf{y}) = d_i\}$ denote the set of points belonging to $C^{\mathbf{H}}$ and surrounding \mathbf{x} at a Euclidean distance d_i . The shape of $S_{\mathbf{x},i}$ is not necessarily spherical due to the cutting boundaries of the constellation. The local theta series is defined by the coefficients $\tau_{\mathbf{x},\ell,i} = |S_{\mathbf{x},i}|$, where $\mathbf{x} \in I_\ell$. The shells in the local theta series are indexed by i in the subscript of τ . The upper bound for $Pe(I_\ell)$ becomes:

$$Pe(I_\ell) \leq \frac{1}{|I_\ell|} \sum_{\mathbf{x} \in I_\ell} \sum_i \tau_{\mathbf{x},\ell,i} \times Q\left(\frac{d_i}{2\sigma}\right). \quad (13)$$

Finally, for a fixed channel matrix \mathbf{H} , an accurate approximation of the point error probability for a multi-dimensional QAM modulation transmitted on a MIMO channel is obtained by combining (13) and

(8)

$$Pe(C^{\mathbf{H}}) \leq \sum_{\ell=0}^n p_\ell \frac{1}{|I_\ell|} \sum_{\mathbf{x} \in I_\ell} \sum_i \tau_{\mathbf{x},\ell,i} \times Q\left(\frac{d_i}{2\sigma}\right). \quad (14)$$

C. Numerical implementation of (14)

The coefficients $\tau_{\mathbf{x},\ell,i}$ of the local theta series are easily determined from the original theta series of the random lattice Λ as follows:

- Step 1: Generate lattice points $\mathbf{y} \in \Lambda$ located at a distance d_i from the origin. These points are found using the *Short Vectors* algorithm based on a Pohst enumeration inside a sphere [14][15][5].
- Step 2: For each \mathbf{y} found in the previous step, check if the translate $\mathbf{y} + \mathbf{x}$ belongs to the constellation $C^{\mathbf{H}}$ and increment $\tau_{\mathbf{x},\ell,i}$ accordingly.

For the derivation of numerical results, we limited the total number of selected points in (14) to $N_x = \min(1000, \prod_{k=1}^{n_t} M_k)$. The number of points selected from the subset I_ℓ (points lying on the intersection of ℓ facets) is weighted by p_ℓ , i.e. we consider $p_\ell N_x$ such points. This method accurately approximates the distribution of constellation points according to their position. The number of shells in the local theta series has been limited to i_{max} , where the most distant shell is at $2d_{Emin}^2(\Lambda)$. The conventional factor 2 is fully justified by its corresponding 3dB signal-to-noise ratio margin on a Gaussian channel. If the local theta series (around \mathbf{x}) is empty, then the new search radius can be increased up to $4d_{Emin}^2(\Lambda)$ (6dB SNR margin).

Another heuristic for controlling i_{max} is to select the initial squared radius greater than $\min_i D_{ii}$, where $[D_{ii}] = \mathbf{G}\mathbf{G}^t$ is the lattice Gram matrix. It can be shown that the minimum Euclidean distance in $C^{\mathbf{H}}$ satisfies

$$d_{Emin}^2(\Lambda) \leq d_{Emin}^2(C^{\mathbf{H}}) \leq \min_{i=1\dots n} D_{ii}. \quad (15)$$

Fig. 4 illustrates the accuracy of (14) in the case of a fixed 4×4 MIMO channel. The point error rate is plotted versus the average signal-to-noise ratio (average SNR assumes that $E[|h_{ij}|^2] = 1$). The matrix \mathbf{H} has been selected at random and kept unchanged for all results shown in Fig. 4. Four different QAM combinations have been tested. The notation 4*M-QAM means that 4 transmit antennas are using M-QAM. When transmitted constellations are not identical, a notation as 16-16-64-64-QAM would mean that $M_1 = M_2 = 16$ and $M_3 = M_4 = 64$. In all cases, computer simulation results below 10^{-1} are very close to the proposed analytical approximation. Fig. 5 illustrates the average error probability of a quasi-static 4×4 MIMO channel with a finite coherence time ($T_c = 10$ instead of $+\infty$). Expectation is made over the distribution of \mathbf{H} in Fig. 5. The proposed approximation is very tight below 10^{-1} .

As shown in Fig. 6, the simple upper bound (6) is less accurate than (14) based on the local theta series. For low SNR, (6) is not necessarily an upper bound because some Voronoi facets are due to more distant

points than those located on the first lattice shell (see the 4*16-QAM case). At high SNR, the influence of those facets is negligible. Also, the gap between the simple bound and the exact error rate decreases with the constellation size at high SNR.

IV. APPLICATION TO ADAPTIVE MODULATION

In adaptive modulation schemes, the transmitter adjusts its parameters (modulation size, transmit power, coding rate, etc) to the current channel state in order to guarantee a target error rate and to achieve the highest possible spectral efficiency. We restrict our scheme to the adaptation of QAM modulation size on each transmit antenna. Power adaptation and coding rate variation are not considered in this paper. CSI is only available at the receiver side. The transmitter is informed via the feedback link about the current QAM adaptation to be applied. The objective of our adaptive modulation scheme is the following: Given an average signal-to-noise ratio per bit, find M_1, M_2, \dots, M_{n_t} in order to maximize $\sum_{k=1}^{n_t} \log_2(M_k)$ under the constraint $Pe(C^H) \leq PER_{target}$, where PER_{target} is the target point error rate. Notice that when $Pe(C^H) \geq PER_{target}$, no data is transmitted and the conditional error probability $Pe(C^H)$ is set to 0. In the latter case, an outage is declared each time $Pe(C^H) \geq PER_{target}$. In practice, if the quality of service depends on the frame error rate (FER) and if a frame has length N_F transmit periods, $N_F \leq T_c$, then $FER = 1 - (1 - PER)^{N_F} \approx N_F \times PER$ for uncoded modulations. The use of channel coding would only modify the relation between FER and PER . Hence, PER_{target} can be easily linked to FER_{target} .

A. A New Adaptive Modulation Scheme

Assume that the n_t -antenna transmitter has N_q distinct QAM modulations. For example, $N_q = 4$ if square constellations 4-QAM, 16-QAM, 64-QAM and 256-QAM are used. If all Tx antennas use the same QAM constellation, then the adaptation scheme should select an optimal solution $(M_1, M_1, \dots, M_1)_{opt}$ among N_q possibilities. If Tx antennas use different QAM constellations, then the adaptation scheme

should select an optimal solution $(M_1, M_2, \dots, M_{n_t})_{opt}$ among $N_q^{n_t}$ possibilities. The adaptive modulation scheme is depicted on Fig. 7.

At the receiver side, the channel estimation block provides \mathbf{H} and σ^2 to the adaptation block. The PER computation function employs (14) to compute $PER = Pe(C^{\mathbf{H}})$, where $C^{\mathbf{H}} = C^{\mathbf{H}}(M_1, M_2, \dots, M_{n_t})$. The final block selects the optimal solution $(M_1, M_2, \dots, M_{n_t})_{opt}$ that maximizes $\sum_{k=1}^{n_t} \log_2(M_k)$ under the guarantee $PER \leq PER_{target}$. Finally, the feedback link conveys $n_t \times \log_2(N_q)$ bits to the transmitter, e.g. 8 feedback bits if $n_t = 4$ and $N_q = 4$.

The complexity of the adaptive scheme depends on the number of modulations to be tested in order to select the optimal one. The poor adaptive modulation when all QAMs are identical, $M_1 = M_2 = \dots = M_{n_t}$, has a low adaptation complexity proportional to N_q . On the contrary, the efficient adaptive modulation when QAM constellations may be distinct per Tx antenna has an adaptation complexity proportional to the number of possibilities, that is equal to $N_q^{n_t}$, e.g. $4^4 = 256$ possibilities if 4 types of QAM are authorized ($M = 4, 16, 64, 256$) with $n_t = 4$ transmit antennas. Hence, a brute force adaptation will cost us $N_q^{n_t}$ numerical evaluation of (14). The spectral efficiency varies from $n_t \times 2$ up to $n_t \times 8$ bits per channel use, e.g. 13 possible values in the interval $[8 \dots 32]$ bits per channel use when $n_t = 4$ antennas and $N_q = 4$. In order to avoid considering the $N_q^{n_t} = 256$ possibilities, a key idea is to select a reduced number of combinations where spectral efficiency is well quantized. We selected a limited number (e.g. 13) of possibilities where all values of spectral efficiencies are represented between $n_t \times 2$ and $n_t \times 8$. The choice of the 13 representative possibilities as in Table I is the first step of adaptation. In the second step of adaptation, each transmit antenna must be assigned to a column in Table I, i.e. we must adequately permute the n_t integers M_k given by the row of Table I selected in the first step. We proposed to assign the M_k 's according to the order of $\|\mathbf{h}_i\|$, where \mathbf{h}_i is the i^{th} row of \mathbf{H} . This is inspired by coded systems. Indeed, if an error-correcting code is used in combination with a soft output decoder, then under the genie

condition (perfect feedback of *a priori* information), the capacities of the n_t independent channels are sorted according to $\|\mathbf{h}_i\|^2$. In our case, QAM modulations are uncoded. Nevertheless, simulation results show that the loss in spectral efficiency with our strategy compared to the brute-force is negligible. The adaptation based on 13 possibilities performs almost exactly as well as 256 possibilities. This strategy reduces the number of QAM combinations from $N_q^{n_t}$ down to $(N_q - 1)n_t + 1$.

For $n_t = N_q = 4$, we sort the transmit antennas such that $\|\mathbf{h}_1\|^2 \leq \|\mathbf{h}_2\|^2 \leq \|\mathbf{h}_3\|^2 \leq \|\mathbf{h}_4\|^2$. Then, we start from the most robust combination (4*4-QAM) upward to the most efficient combination (4*256-QAM) as shown in Table I. Only one integer is changed from one row to another according to a decreasing order of Tx antennas power. Consequently, thanks to the dichotomy method applied on the reduced list, a maximum of 4 evaluations of $Pe(C^{\mathbf{H}})$ are required instead of $N_q^{n_t} = 256$.

B. Computer Simulation of the Adaptive Modulation

The considered target point error rate is $PER_{target} = 10^{-3}$. The QAM selection is made as in the reduced list given in Table I. Fig. 8 presents the performance of a 4×4 antenna system satisfying the constraint on the error probability for each channel \mathbf{H} and each noise variance, *i.e.* $Pe(C^{\mathbf{H}}) \leq PER_{target}$. Clearly, the curves corresponding to both non adaptive and adaptive schemes are below the target. The upper curve corresponding to adaptive modulation is close but less than the 10^{-3} target. It also shows a good stability within a 10dB signal-to-noise ratio range. For high noise variance, the selected combination corresponds to the lowest one (*i.e.* 4*4-QAM) for the majority of channels. On the other hand, PER of the adaptive scheme tends to that of 4*256-QAM at high SNR. Fig. 9 represents the probability of no transmission (known as *outage probability*), *i.e.* $Pe(C^{\mathbf{H}}) > PER_{target}$. The outage probability of the adaptive modulation is superimposed with the outage of a fixed 4*4-QAM modulation. Therefore, the proposed adaptive modulation is as robust as the 4-QAM but it guarantees a higher spectral efficiency. It leads to a maximization of the spectral efficiency while keeping the error probability close to the target.

In Fig. 10, the total spectral efficiency achieved by a 4×4 antenna system is presented versus the

average received SNR while satisfying the PER constraint. This figure also emphasizes the advantage of adaptive modulation. The stair including 4 soft steps corresponds to the non adaptive scheme when all Tx antennas are using the same QAM constellation. Albeit the looseness of (6) shown in Fig. 6, the adaptive modulation based on minimum Euclidean distance exhibits a small spectral efficiency loss at low SNR with respect to adaptation based on local theta series.

V. CONCLUSIONS

An accurate approximation for the conditional error probability on quasi-static multiple antenna channels has been described. For a fixed channel matrix \mathbf{H} , it is possible to accurately predict the performance of QAM modulations transmitted over the MIMO channel in presence of additive white Gaussian noise. The approximation is based on a tight Union bound for the point error probability in the n -dimensional real space. Instead of making an exhaustive evaluation of all pairwise error probabilities (intractable even for moderate values of n_t and M), a Pohst lattice enumeration is used to limit the local theta series inside a finite radius sphere. The local theta series is derived from the original lattice theta series and the point position within the finite multi-dimensional QAM constellation. As a direct application, we also described an adaptive QAM modulation scheme for quasi-static MIMO channels.

REFERENCES

- [1] E. Agrell, T. Eriksson, A. Vardy, and K. Zeger, "Closest point search in lattices," *IEEE Trans. on Inf. Theory*, vol. 48, no. 8, pp. 2201-2214, Aug. 2002.
- [2] E. Biglieri, G. Taricco, and A. Tulino, "Decoding space-time codes with BLAST architecture," *IEEE Trans. on Signal Processing*, vol. 50, no. 10, pp. 2547-2552, Oct. 2002.
- [3] J. Boutros, N. Gresset, L. Brunel, and M. Fossorier, "Soft-input soft-output lattice sphere decoder for linear channels," *IEEE Global Communications Conference*, vol. 3, pp. 1583-1587, San Francisco, Dec. 2003.
- [4] J. Boutros, E. Viterbo, C. Rastello, and J.C. Belfiore, "Good lattice constellations for both Rayleigh fading and Gaussian channels," *IEEE Trans. on Information Theory*, vol. 42, no. 2, pp. 502-518, March 1996.
- [5] H. Cohen: *Computational algebraic number theory*, Springer Verlag, 1993.
- [6] J. H. Conway and N. J. Sloane: *Sphere packings, lattices and groups*, 3rd edition, Springer-Verlag, New York, 1998.

- [7] T. Cui and C. Tellambura, "An efficient generalized sphere decoder for rank-deficient MIMO systems," *IEEE Communications Letters*, vol. 9, no. 5, pp. 423-425, May 2005.
- [8] G. D. Forney, "Coset codes I: introduction and geometrical classification," *IEEE Trans. on Information Theory*, vol. 34, no. 5, pp. 1123-1151, Sept. 1988.
- [9] G.J. Foschini and M.J. Gans, "On limits of wireless communication in a fading environment when using multiple antennas," *Wireless Personal Communications*, vol. 6, no. 3, pp. 311-335, Mar. 1998.
- [10] A.J. Goldsmith and S.-G. Chua, "Variable-rate variable-power M-QAM for fading channels," *IEEE Transactions on Communications*, vol. 45, no. 10, pp. 1218-1230, Oct. 1997.
- [11] S.T. Chung and A.J. Goldsmith, "Degrees of freedom in adaptive modulation: a unified view," *IEEE Transactions on Communications*, vol. 49, no. 9, pp. 1561-1571, Sept. 2001.
- [12] R.W. Heath, S. Sandhu, and A. Paulraj, "Antenna selection for spatial multiplexing systems with linear receivers," *IEEE Communications Letters*, vol. 5, no. 4, pp. 142-144, April 2001.
- [13] R.W. Heath and A. Paulraj, "Antenna selection for spatial multiplexing systems based on minimum error rate," *IEEE International Conference on Communications*, vol. 7, pp. 2276-2280, June 2001.
- [14] M. Pohst, "On the computation of lattice vectors of minimal length, successive minima and reduced bases with applications," *ACM SIGSAM Bull.*, vol. 15, pp.37-44, 1981.
- [15] M. Pohst and H. Zassenhaus, *Algorithmic algebraic number theory*, Encyclopedia of Mathematics and its Applications, Cambridge University Press, 1989.
- [16] J. Proakis, *Digital Communications*, 4th edition, McGrawHill, New York, 2000.
- [17] P. Sebastian, H. Sampath, and A. Paulraj, "Adaptive modulation for multiple antenna systems," *Asilomar Conf. on Signals, Systems and Computers*, vol. 1, pp. 506-510, Oct. 2000.
- [18] G. Taricco and E. Biglieri, "Exact pairwise error probability of space-time codes," *IEEE Trans. on Inf. Theory*, vol. 48, no. 2, pp. 510-513, Feb. 2002.
- [19] G. Taricco and E. Biglieri, "Correction to exact pairwise error probability of space-time codes," *IEEE Trans. on Inf. Theory*, vol. 49, no. 3, pp. 766-766, March 2003.
- [20] V. Tarokh, N. Seshadri, and A.R. Calderbank, "Space-time codes for high data rate wireless communication: performance criterion and code construction," *IEEE Trans. on Inf. Theory*, vol. 44, no. 2, pp. 744-765, March 1998.
- [21] V. Tarokh, Alexander Vardy, and Kenneth Zeger, "Universal Bound on the Performance of Lattice Codes," *IEEE Trans. on Inf. Theory*, vol. 45, no. 2, pp. 670-681, March 1999.
- [22] I.E. Telatar, "Capacity of multi-antenna Gaussian Channels," *European Trans. on Telecomm.*, vol. 10, no. 6, pp. 585-595, Nov.-Dec. 1999.
- [23] E. Viterbo and J. Boutros, "A universal lattice code decoder for fading channels," *IEEE Trans. on Inf. Theory*, vol. 45, no. 5, pp. 1639-1642, July 1999.

- [24] E. Viterbo and E. Biglieri, "Computing the Voronoi cell of a lattice: the diamond-cutting algorithm," *IEEE Trans. on Inf. Theory*, vol. 42, no. 1, pp. 161-171, Jan. 1996.

TABLE I
 REDUCED LIST FOR ADAPTIVE MODULATION, $N_q = 4$ DISTINCT QAM SETS AND $n_t = 4$ TX ANTENNAS.

Tx 1	Tx 2	Tx 3	Tx 4
256	256	256	256
			highest spectral efficiency worst error rate performance
64	256	256	256
64	64	256	256
64	64	64	256
64	64	64	64
16	64	64	64
16	16	64	64
16	16	16	64
16	16	16	16
4	16	16	16
4	4	16	16
4	4	4	16
4	4	4	4
			lowest spectral efficiency best error rate performance

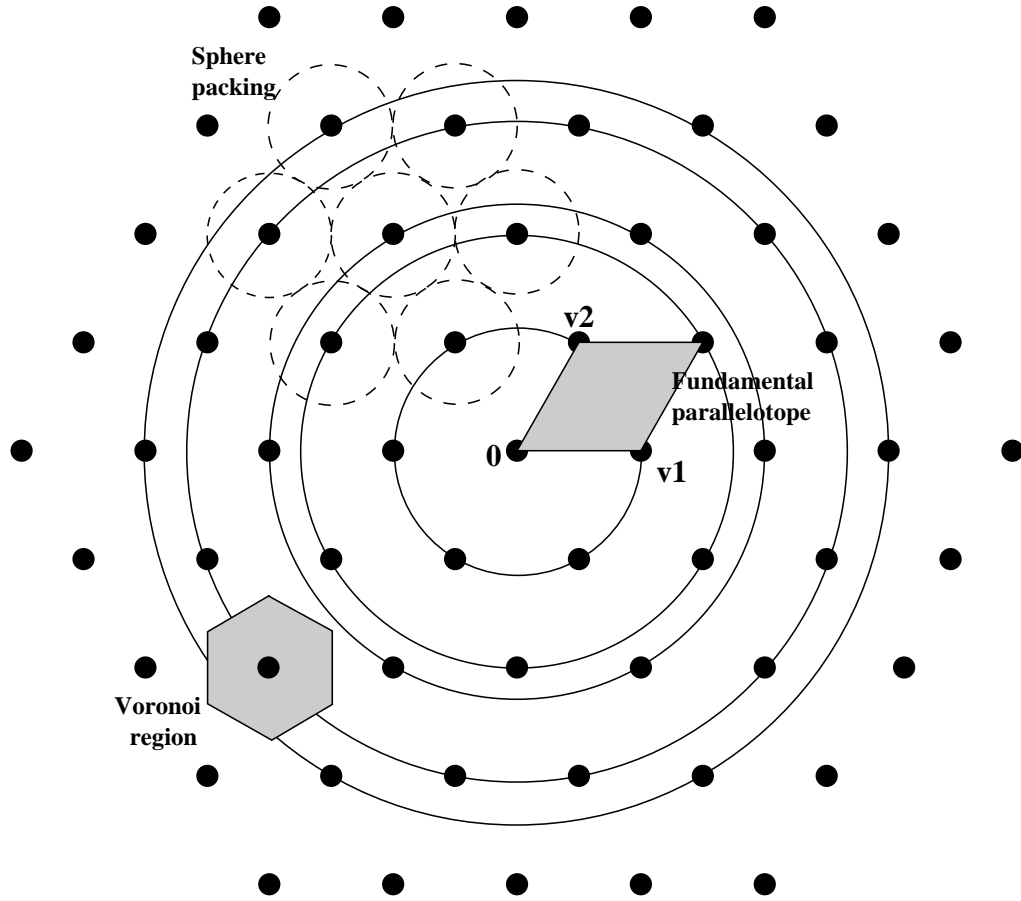


Fig. 1. Structure of the hexagonal lattice A_2 in the real bidimensional space. MIMO lattices are random, but their structure can be determined by number theoretical algorithms.

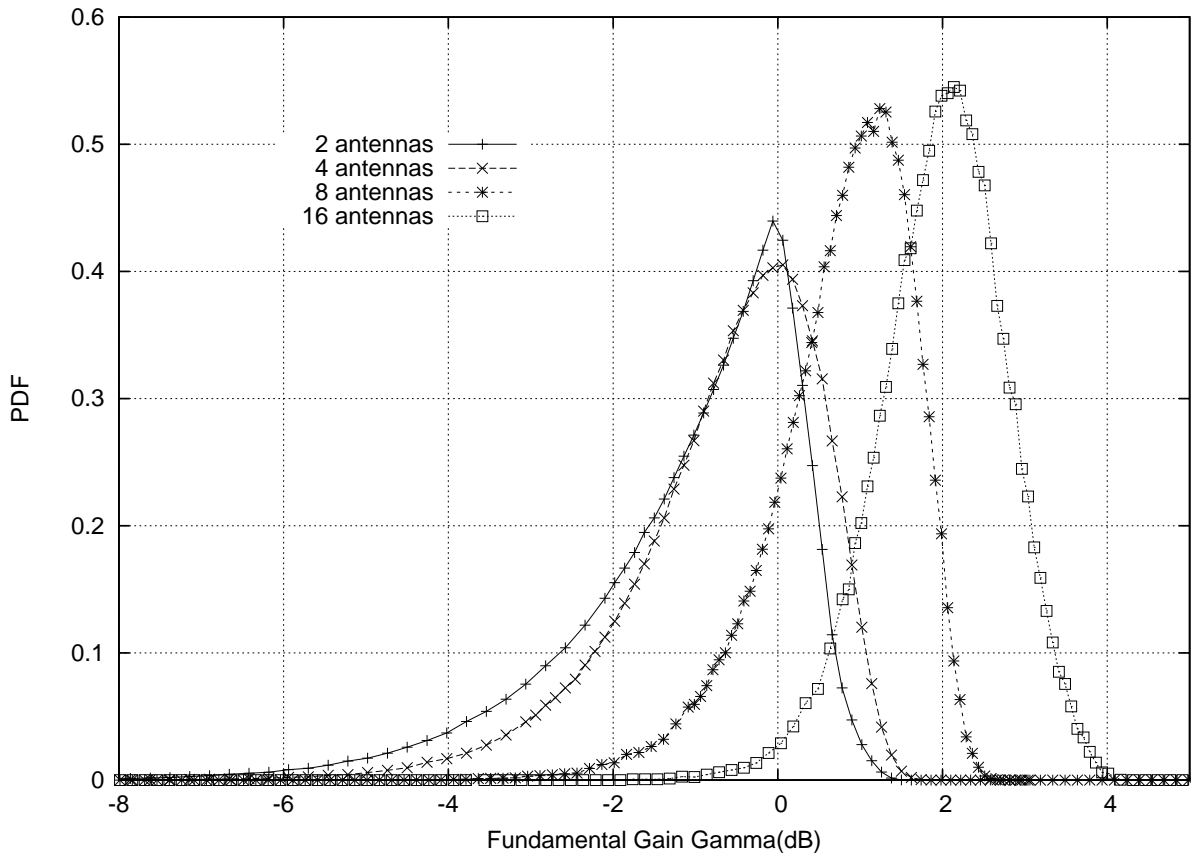


Fig. 2. Distribution of the lattice fundamental gain γ (dB) (Hermite constant) in a symmetric MIMO channel $n_t = n_r$.

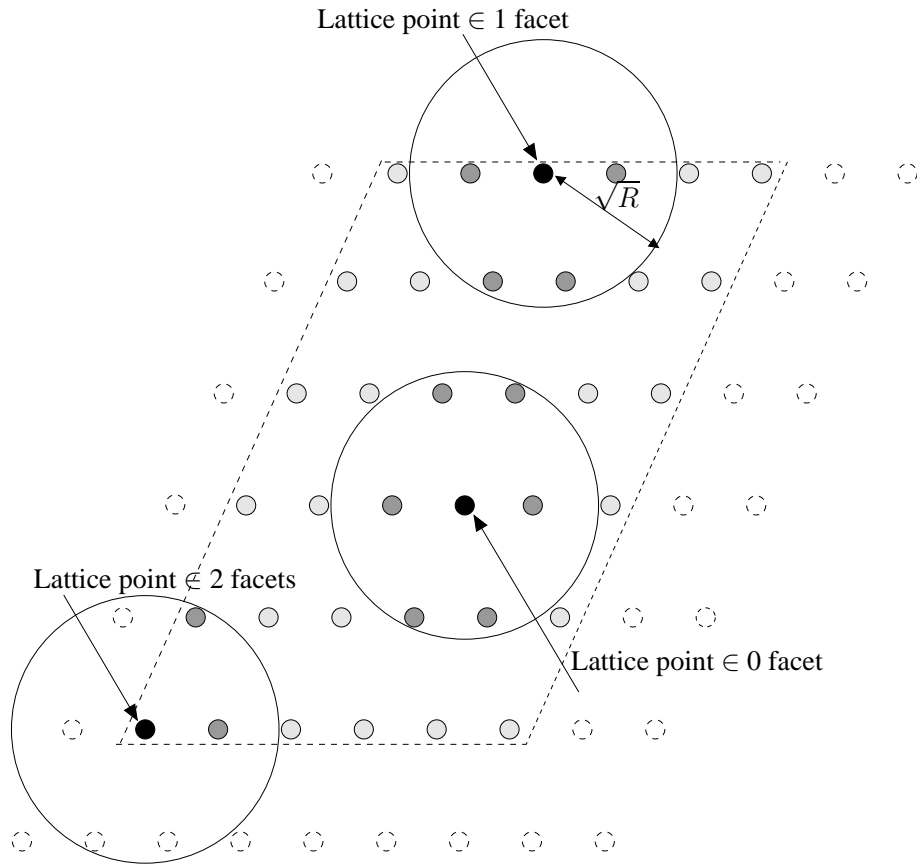


Fig. 3. An example of lattice constellation in \mathbb{R}^2 . Points are distinguished according to the number of crossing facets.

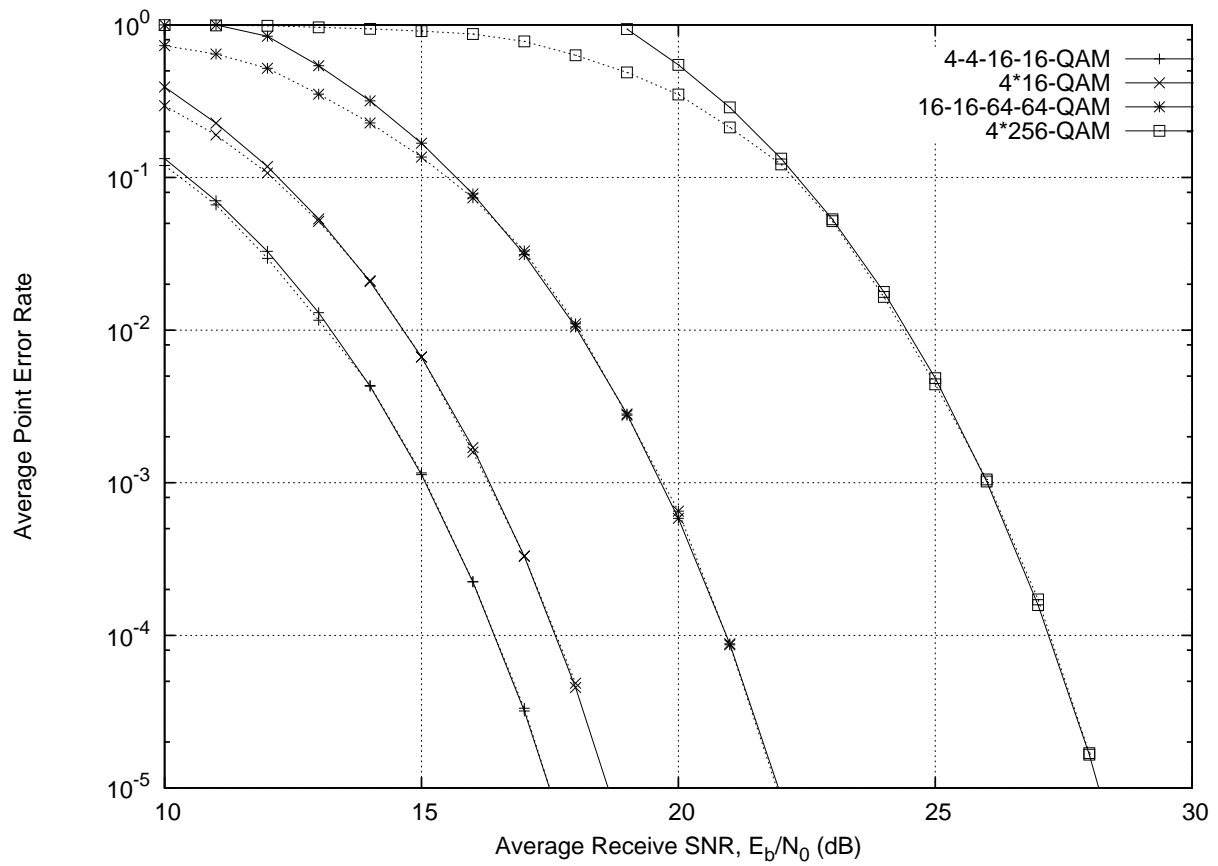


Fig. 4. Error probability of a 4×4 static MIMO channel ($T_c = +\infty$). Analytic approximation (continuous lines) and Monte Carlo simulation (dotted lines).

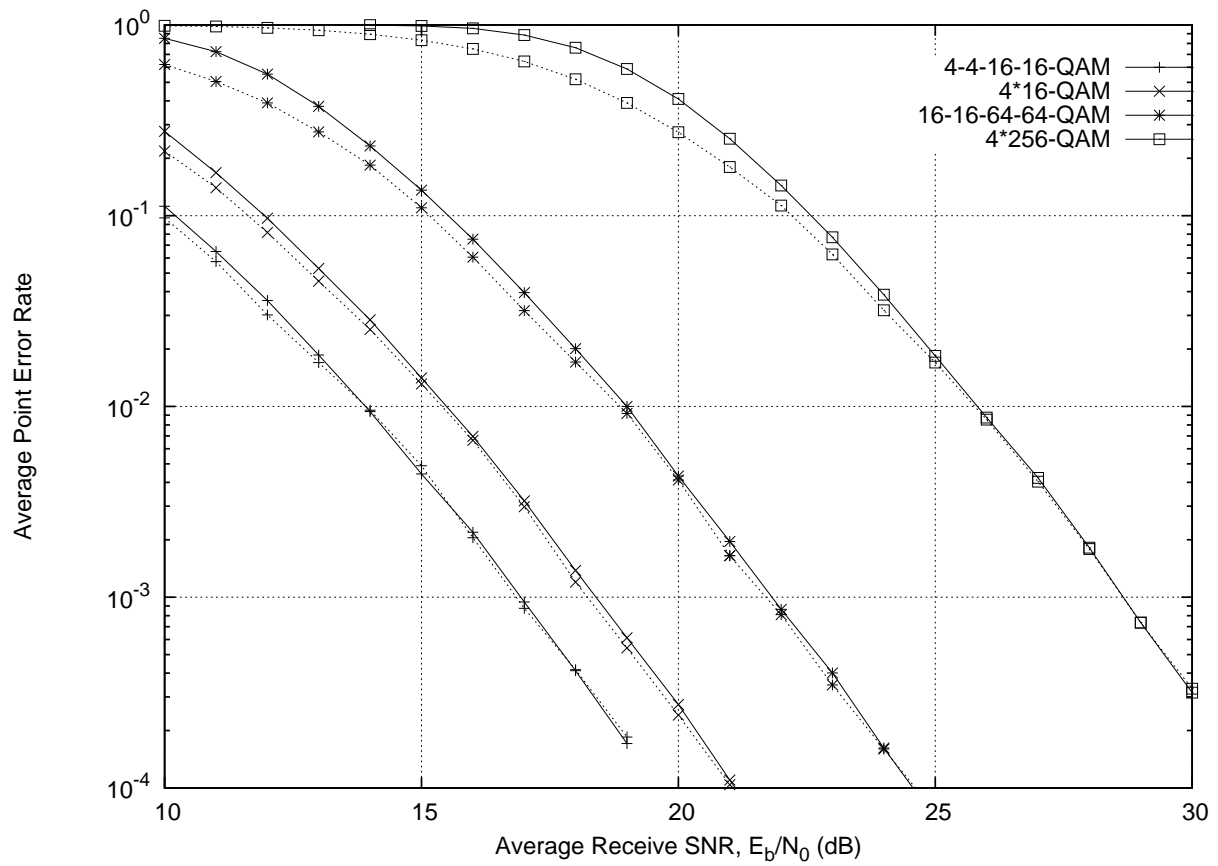


Fig. 5. Average error probability of a 4×4 quasi-static MIMO channel ($T_c = 10$). Analytic approximation (continuous lines) and Monte Carlo simulation (dotted lines).

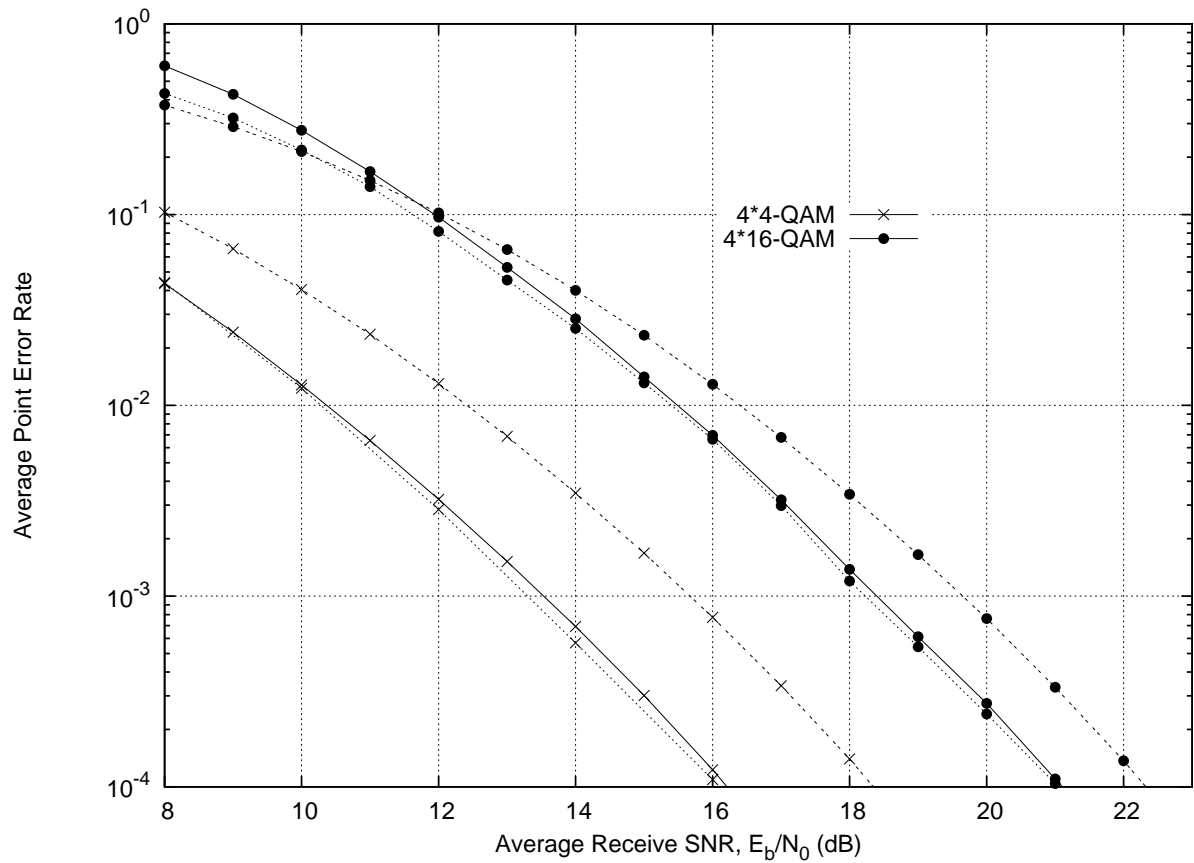


Fig. 6. Average error probability of a 4×4 quasi-static MIMO channel ($T_c = 10$). Analytic approximation given in (14) based on local theta series (continuous lines), bound given in (6) based on minimum Euclidean distance (dashed lines), and Monte Carlo simulation (dotted lines).

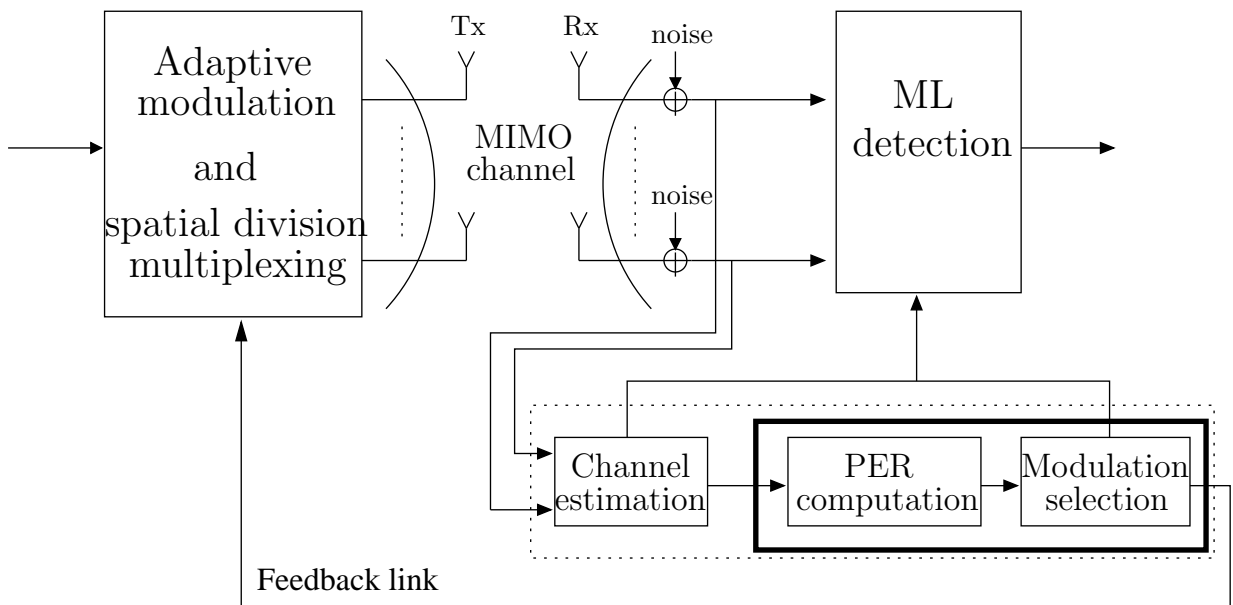


Fig. 7. Adaptive QAM modulation receiver/transmitter pair for quasi-static MIMO channels.

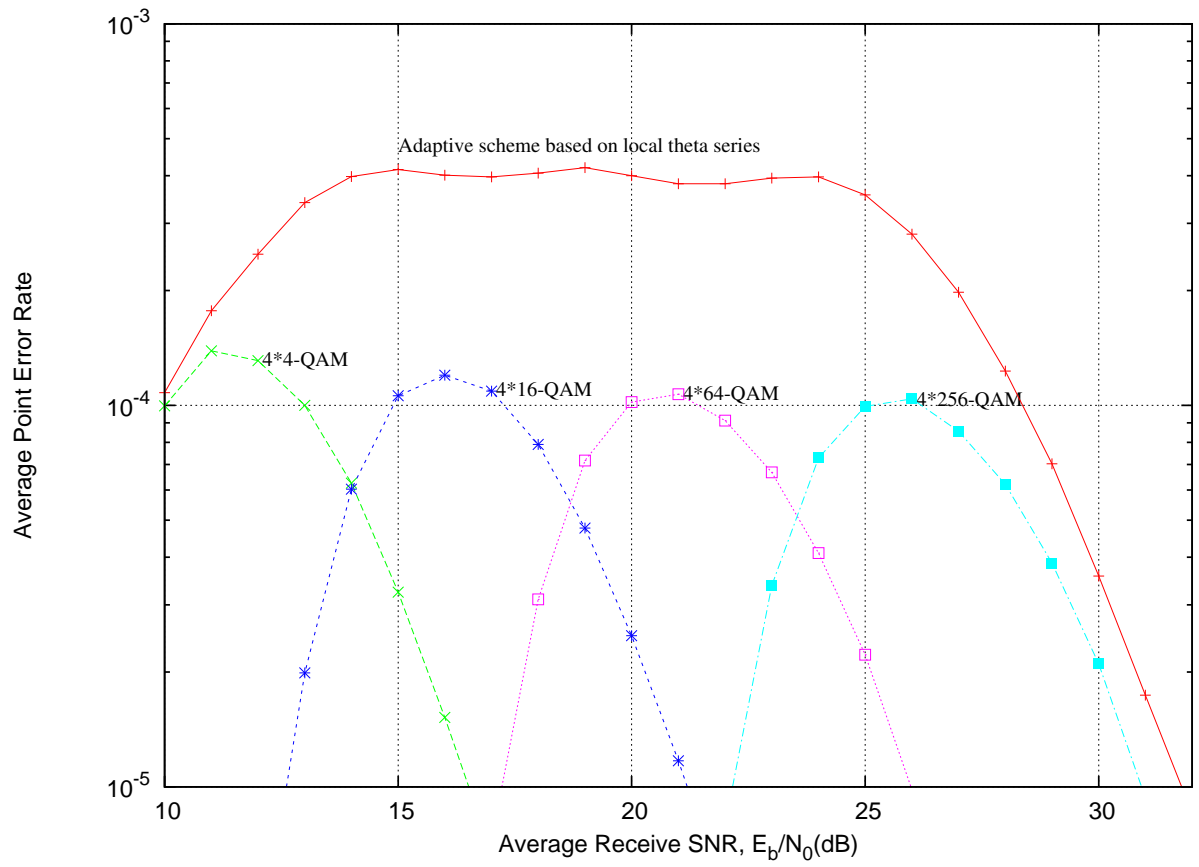


Fig. 8. Point error rate function of average signal-to-noise ratio, adaptive versus non-adaptive modulation policy, 4×4 quasi-static MIMO channel.

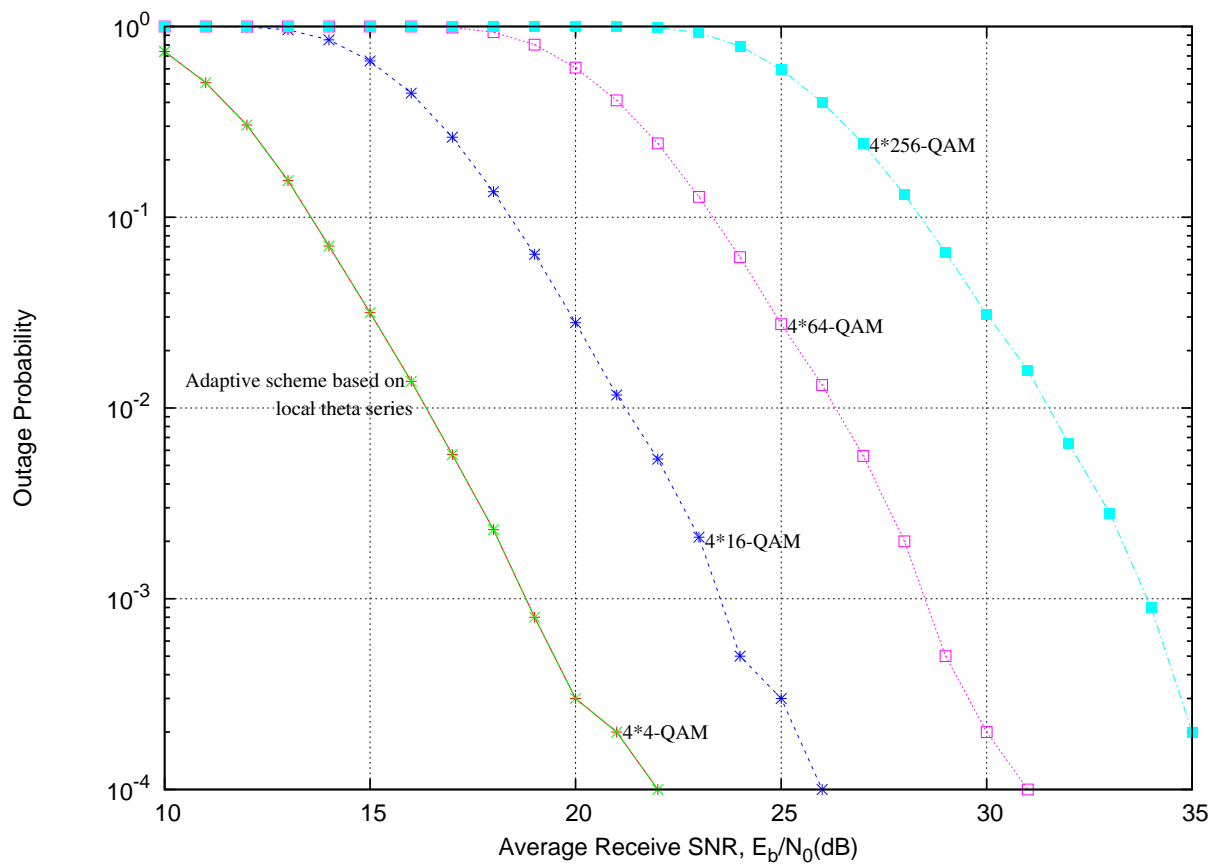


Fig. 9. Outage probability versus average signal-to-noise ratio, 4×4 quasi-static MIMO channel. No transmission if $Pe(C^H) > Pe_{target}$.

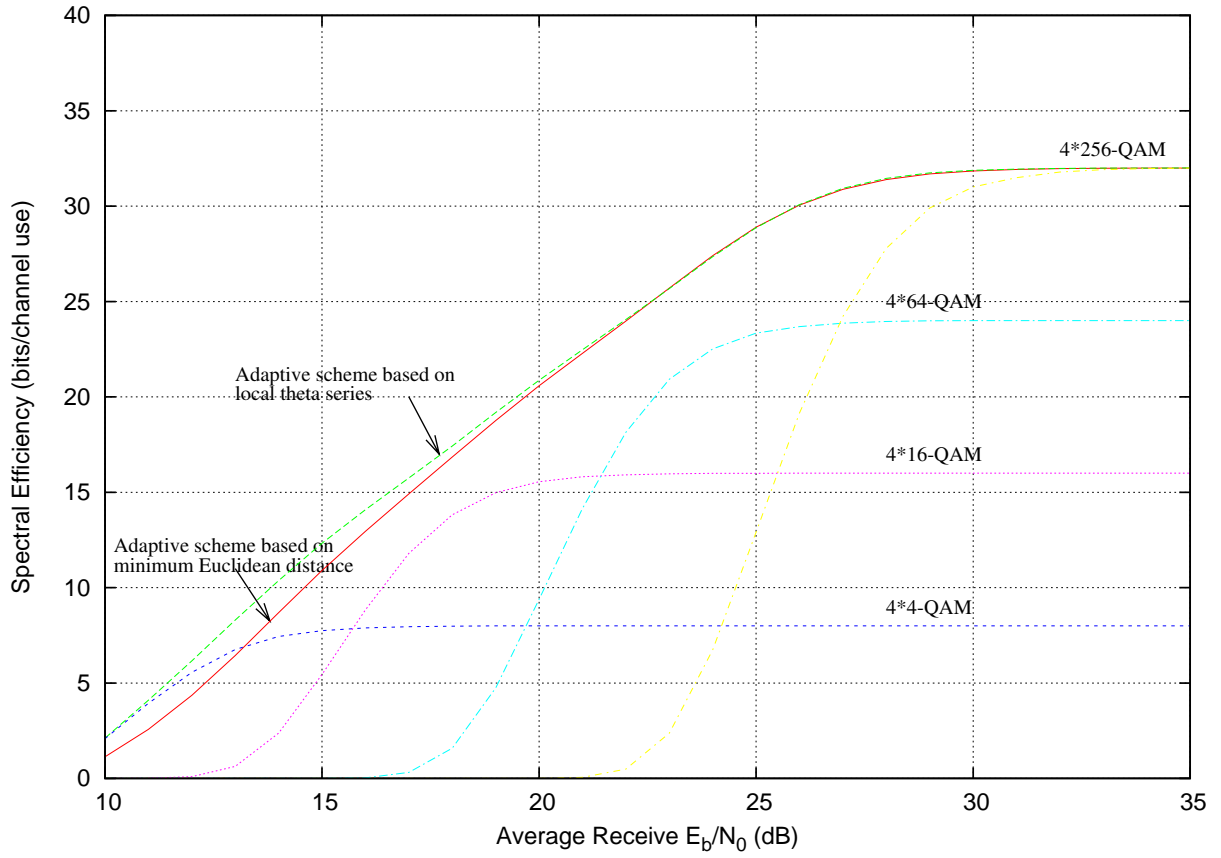


Fig. 10. Spectral efficiency of adaptive modulation versus non-adaptive scheme, 4×4 quasi-static MIMO channel.